Electronic Supplementary Material (ESI) for Physical Chemistry Chemical Physics.

Supplementary Materials for Superconductivity in Ca-intercalated bilayer graphene: C_2CaC_2

Jin-Han Tan[1], Hao Wang[1], Ying-Jie Chen[1], Na Jiao[1],
Meng-Meng Zheng[1*], Hong-Yan Lu[1*] and Ping Zhang[1,2*]
[1]School of Physics and Physical Engineering, Qufu Normal University, Qufu 273165, China
[2] Institute of Applied Physics and Computational Mathematics, Beijing 100088, China.

Corresponding Authors
*E-mail:(M. M. Z.) qfzhmm@163.com
*E-mail:(H. Y. L.) hylu@qfnu.edu.cn
*E-mail:(P. Z.) zhang_ping@iapcm.ac.cn

I. Computational details.

The total EPC constant λ is obtained via isotropic Eliashberg function [1–3]:

$$\alpha^2F(\omega) = \frac{1}{2\pi N(E_F)} \sum_{q\nu} \delta(\omega - \omega_{q\nu}) \frac{\gamma_{q\nu}}{\omega_{q\nu}}, \quad (1)$$

$$\lambda = 2\int_0^{\infty} \frac{\alpha^2F(\omega)}{\omega} d\omega = \sum_{q\nu} \lambda_{q\nu}, \quad (2)$$

where $\alpha^2F(\omega)$ is Eliashberg function and $N(E_F)$ is the DOS at the Fermi level, $\omega_{\mathbf{q}\nu}$ is the phonon frequency of the νth phonon mode with wave vector $\mathbf{q}$, and $\gamma_{\mathbf{q}\nu}$ is the phonon linewidth [1–3]. The $\gamma_{\mathbf{q}\nu}$ can be estimated by:

$$\gamma_{q\nu} = \frac{2\pi\omega_{q\nu}}{\Omega_{BZ}} \sum_{k,n,m} \left| g^{\nu}_{kn,\,k+qm} \right|^2 \delta(\varepsilon_{kn} - E_F) \delta(\varepsilon_{k+qm} - E_F), \quad (3)$$

where $\mathbf{\Omega}_{\mathrm{BZ}}$ is the volume of the Brillouin zone (BZ), $\varepsilon_{\mathbf{k}n}$ and $\varepsilon_{\mathbf{k}+\mathbf{q}m}$ indicate the Kohn-Sham energy, and $g^{\nu}_{\mathbf{k}n,\mathbf{k}+\mathbf{q}m}$ represents the screened electron-phonon matrix element. $\lambda_{\mathbf{q}\nu}$ is the EPC constant for phonon mode $\mathbf{q}\nu$, which is defined as:

$$\lambda_{q\nu} = \frac{\gamma_{q\nu}}{\pi\hbar N(E_F)\omega^2_{q\nu}}. \quad (4)$$

T_c is estimated by the Allen-Dynes modifified McMillan equation [3]:

$$T_c = \frac{\omega_{log}}{1.2} exp\left[\frac{-1.04(1+\lambda)}{\lambda - \mu^*(1+0.62\lambda)}\right]. \quad (5)$$

The hysteretic Coulomb pseudopotential μ^* in Eq. (5) is set to 0.1 and logarithmic average of the phonon frequencies $\omega_{\log}$ is defined as:

$$\omega_{log} = exp\left[\frac{2}{\lambda}\int_0^{\omega} \alpha^2F(\omega)\frac{log\omega}{\omega} d\omega\right]. \quad (6)$$

II. The crystal structure of Ca-intercalated AB-stacking bilayer graphene C_2CaC_2.

The lattice structure of calcium intercalated AB-stacking bilayer graphene C_2CaC_2 is shown in Fig. S1. After full optimization, the lattice parameter is 2.59 Å, which is slightly smaller than that of the AA-stacking C_2CaC_2. The height between the two graphene layers is 5.294 Å, slightly larger than that of the AA-stacking C_2CaC_2. When calculating its stability, we find that its phonon dispersion has no imaginary frequencies, as shown in Fig. S2, indicating dynamic stability. However, during the subsequent verification of thermodynamic stability, it gradually changed to AA-stacking with lower system energy, as shown in Fig. S3.

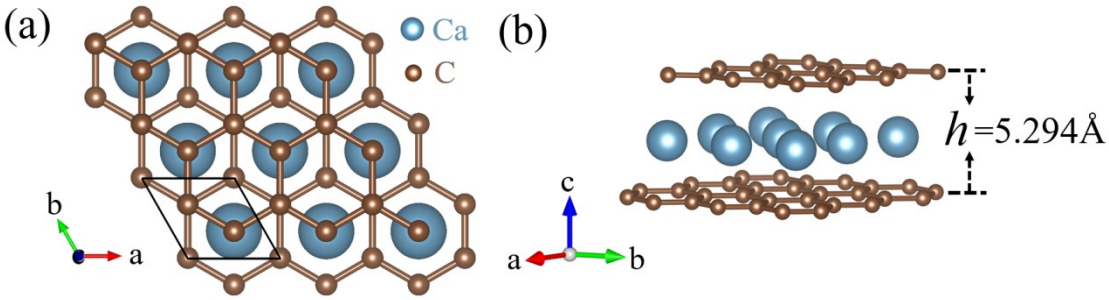

FIG. S1 (a) Top (a) and side (b) views of Ca-intercalated AB-stacking bilayer graphene C_2CaC_2. The unit cell is shown by the black solid line. Carbon, calcium atoms are represented by brown and blue spheres, respectively.

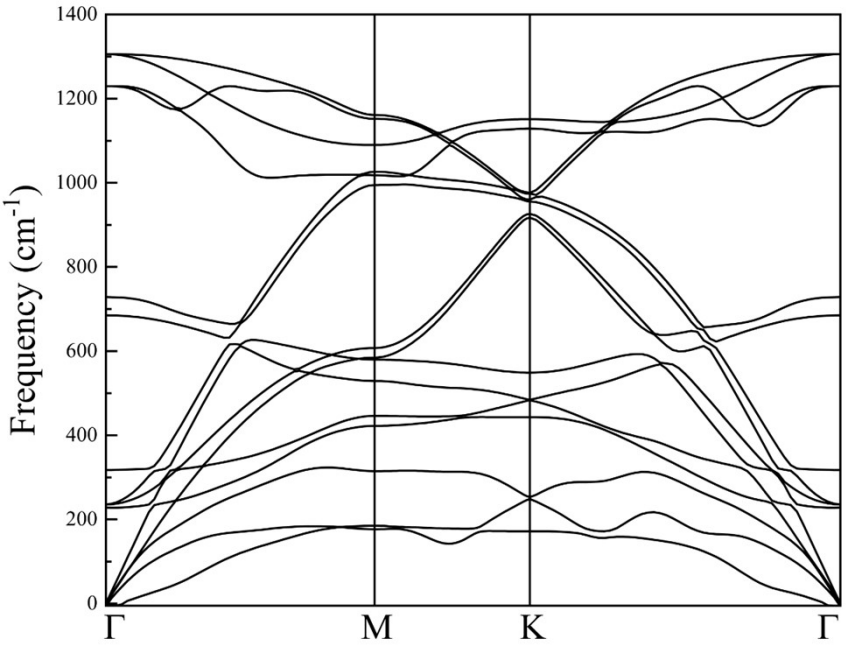

FIG. S2 Phonon dispersion for the AB-stacking C_2CaC_2.

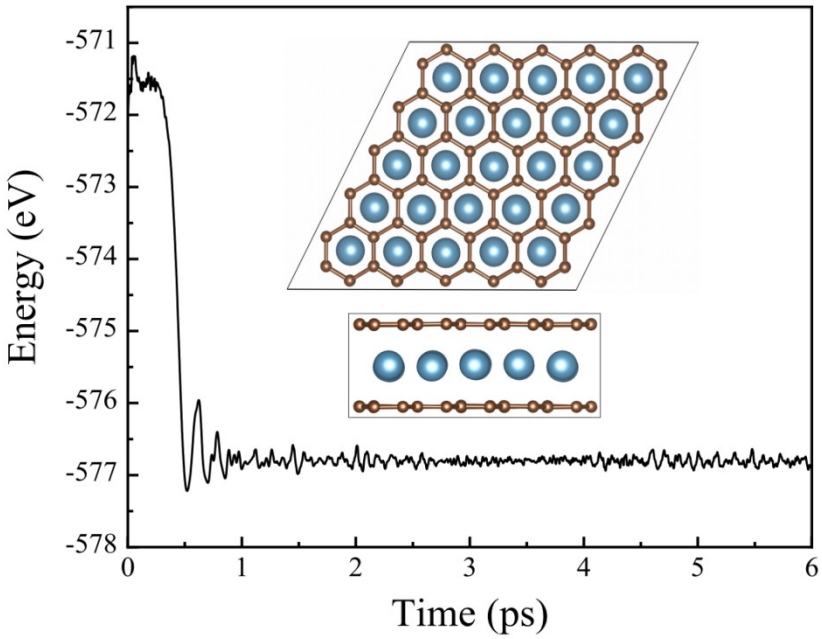

FIG. S3 The variation of the free energy in the AIMD simulations in the time scale of 6 ps along with the last frame of photographs at 50 K for the AB-stacking C_2CaC_2.

III. The calculated phonon dispersion of C_2CaC_2 in the case of biaxial strain with ε = -7%, 11%.

In the case of different strained cases applied to the structure, we find that with ε = -7% and 11% of C_2CaC_2, the structure begins to show dynamic instability. As is shown in Fig. S4, the phonon dispersion exhibits imaginary frequencies.

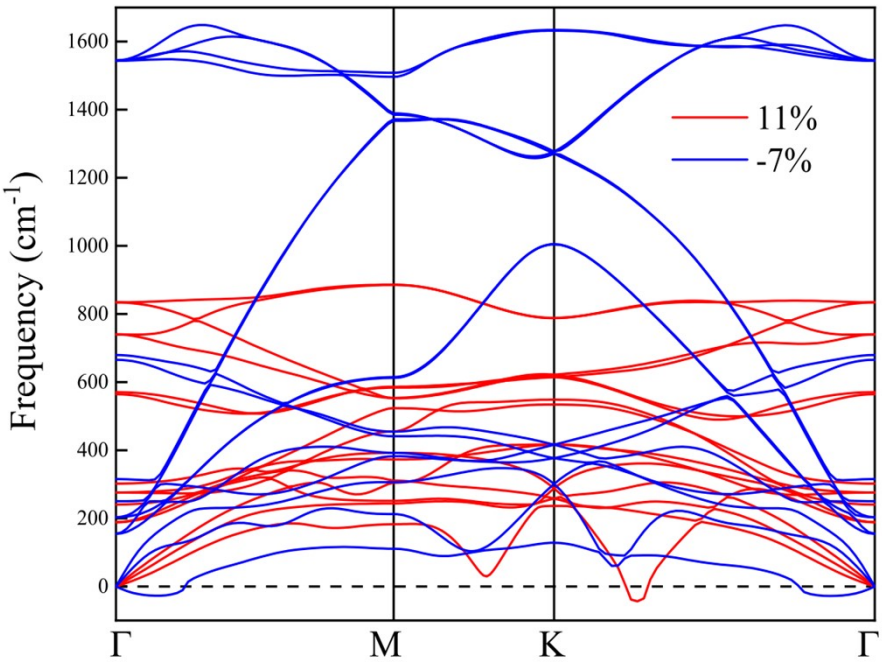

FIG. S4 Phonon dispersion of C_2CaC_2 in the case of biaxial strain with ε = 11% and -7%.

IV. The T_c of pristine calcium intercalated AA-stacking bilayer graphene C_2CaC_2 and biaxial compressive strained C_2CaC_2 as a function of Coulomb pseudopotential μ*.

It is well known that the Coulomb pseudopotential μ* is an empirical parameter which is closely associated with T_c. The calculated T_c of pristine calcium intercalated AA-stacking bilayer graphene C_2CaC_2 and biaxial tensile strained C_2CaC_2 as a function of μ* is shown in Fig. S5. The value of μ* is considered in the range of 0.05–0.20. As is seen in Fig. S5, the T_c decreases monotonically with the increasing of μ* for both pristine C_2CaC_2 and biaxial tensile strained C_2CaC_2. As μ* increases from 0.05 to 0.20, T_c decreases from 26.3 K, 28.6 K, 32.2 K to 7.1 K, 10.3 K, 16.1 K for the pristine, -2% and -4% compressive strained cases, respectively. For the commonly used μ* = 0.10, the T_c for the pristine, -2% and -4% compressive strained cases are 18.9 K, 21.9 K and 26.6 K, respectively, which are listed in Table 1 of the main text.

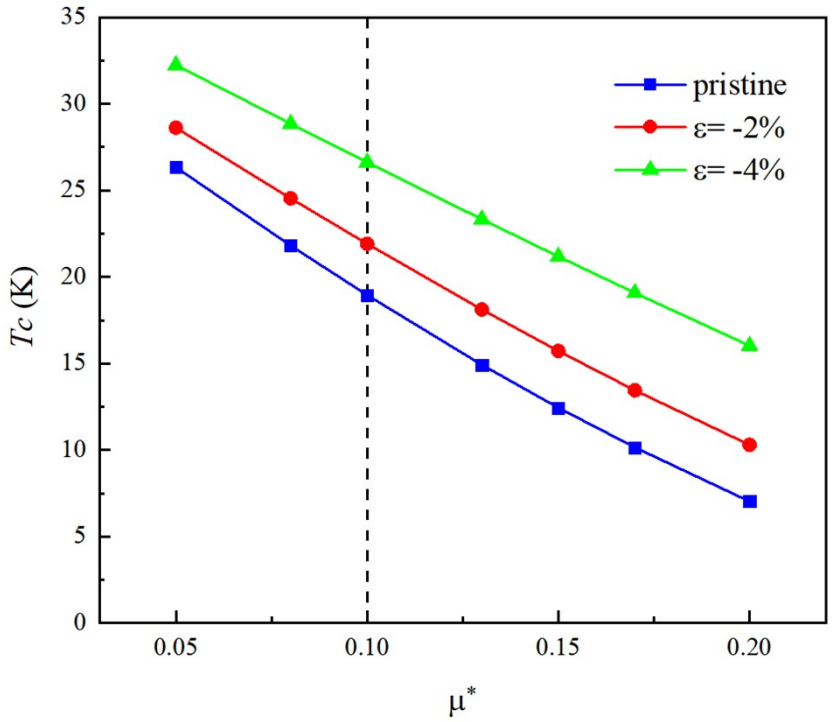

FIG. S5: The calculated *Tc* of pristine calcium intercalated AA-stacking bilayer graphene C_2CaC_2 and biaxial tensile strained C_2CaC_2 as a function of Coulomb pseudopotential μ*. The vertical line marks the value of μ* = 0.10 used in the main text.

V. The λ and T_c as a function of degauss for different *k* meshes and *q* meshes for pristine C_2CaC_2.

The convergence of T_c is consistent with the convergence of the EPC λ, which should satisfy two requirements: (1) λ/T_c should converge with respect to the k mesh and q mesh, that is, for a dense enough *k* mesh and *q* mesh, the λ vs degauss curve should become overlap. (2) λ/T_c should also converge with degauss (the smearing width in the EPC calculation). We should find the degauss at which λ/T_c becomes relatively flat, and the results at this degauss should be chosen as the convergence data. To test the convergence of the λ and T_c of pristine C_2CaC_2, we plot the curves for λ and T_c under a series of degauss with *k* meshes of 24 × 24 × 1, 32 × 32 × 1, and 48 × 48 × 1 and corresponding *q* meshes of 4 × 4 × 1, 8 × 8 × 1, and 12 × 12 × 1, which are shown by the black, red, and blue lines with squares, dots, and triangles in Fig. S6. From Figs. S6(a) and S6(b), we can find the following results: (1) Using different *k* meshes and *q* meshes, the corresponding λ basically converges at *k* mesh of 48 × 48 × 1 and the corresponding *q* mesh of 12 × 12 × 1. (2) The T_c also converges at this *k* mesh and *q* mesh, and the T_c vs degauss curve becomes relatively flat at degauss of 0.015 Ry, with a corresponding T_c of 18.9 K. Thus, the *k* mesh and *q* mesh used in this work is converged for the calculation of T_c.

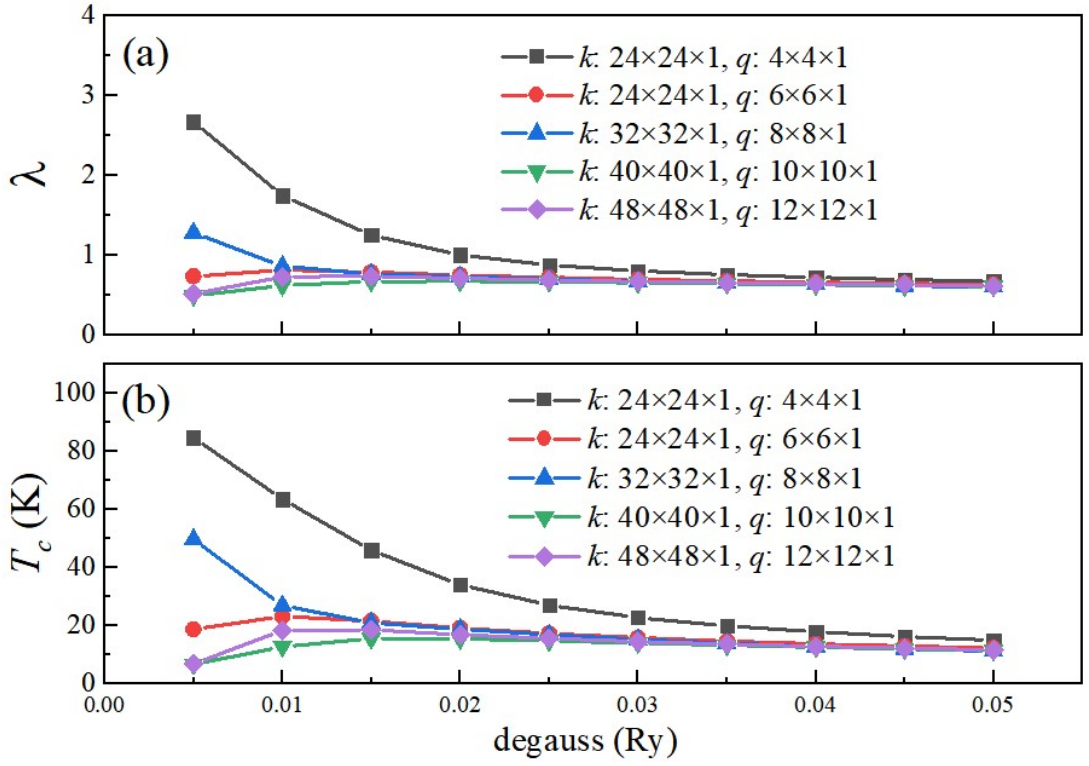

Fig. S6: λ(a) and T_c (b) as a function of degauss for different *k* meshes and *q* meshes for pristine C_2CaC_2.

VI. The phonon spectrum corresponding to different smearing parameter for pristine C_2CaC_2.

Using Methfessel-Paxton smearing method for the electronic charge density calculations, it is important to select critical smearing parameter as it significantly impacts the imaginary phonon modes. In addition to the 0.02 parameter used in the paper, we also calculated the phonon dispersion for parameters 0.01 and 0.03 and found no imaginary frequency. Figs. S7(a) and S7(b) represent phonon spectra with parameters 0.01 and 0.03, respectively.

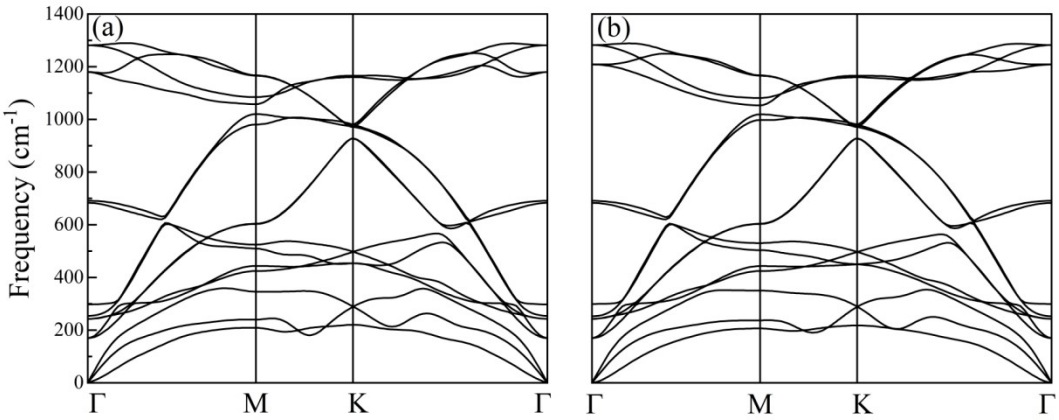

Fig. S7: The phonon dispersion with smearing parameters 0.01 (a) and 0.03 (b) of pristine C_2CaC_2.

VII. Electron localization function (ELF) of pristine C_2CaC_2.

The ELF value ranges from 0 to 1. Generally, 0 indicates very low electron density, 0.5 indicates homogeneity of electron gas, and 1 indicates strong covalent bonding or lone pair electrons. The 2D maps of ELF for C_2CaC_2 are shown in Fig. S8. The ELF value between C and Ca is almost zero, indicating a very low electron density as shown in Fig. S8(a). That suggested ionic bond between C and Ca atoms. Fig. S8(b) suggested covalent bonds between C atoms.

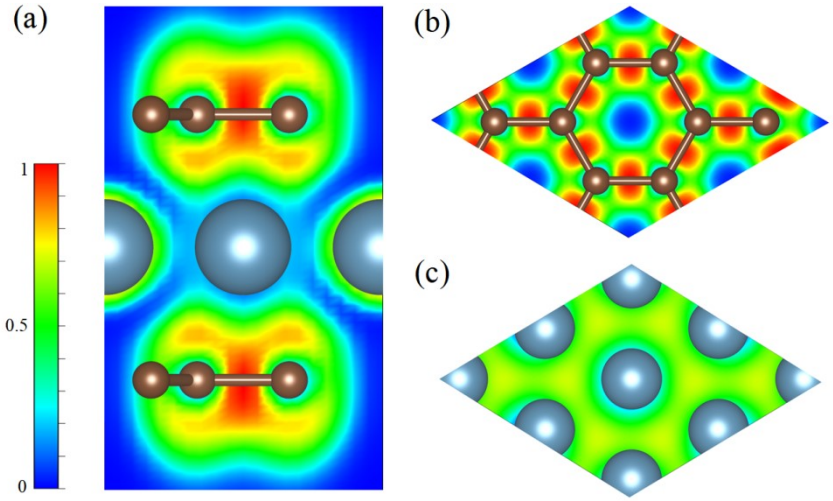

Fig. S8: 2D maps of ELF for C_2CaC_2.

References

[1] W. L. McMillan, *Phys. Rev.*, 1968. **167**, 331.
[2] R.C. Dynes, *Solid State Commun.*, 1972, **10**, 615.
[3] P.B. Allen and R.C. Dynes, *Phys. Rev. B*, 1975, **12**, 905.